DOI: 10.1002/chem.200600965

Magnetic transmission through ligands

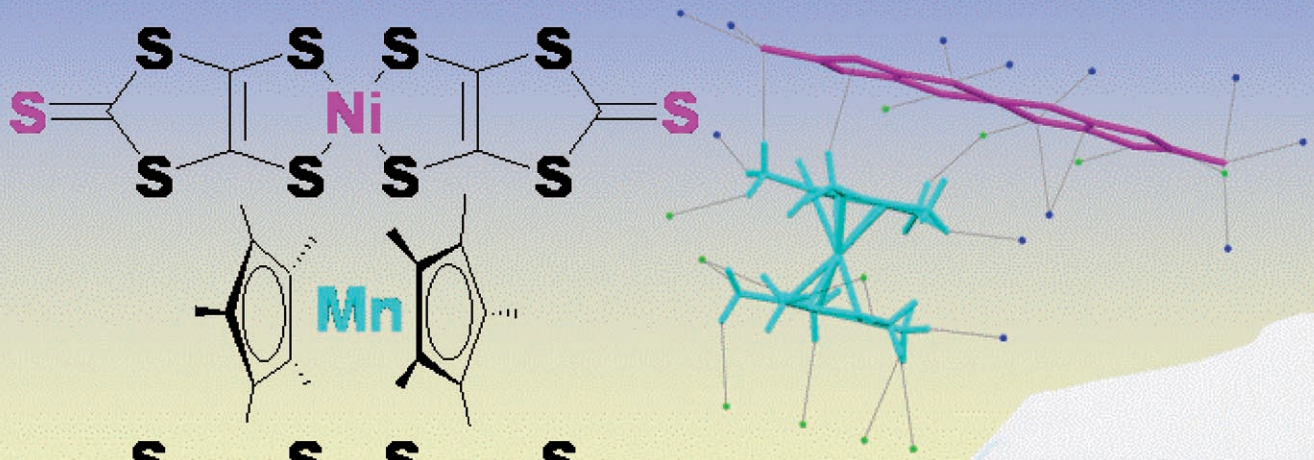

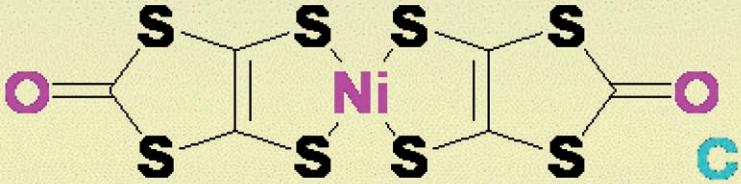

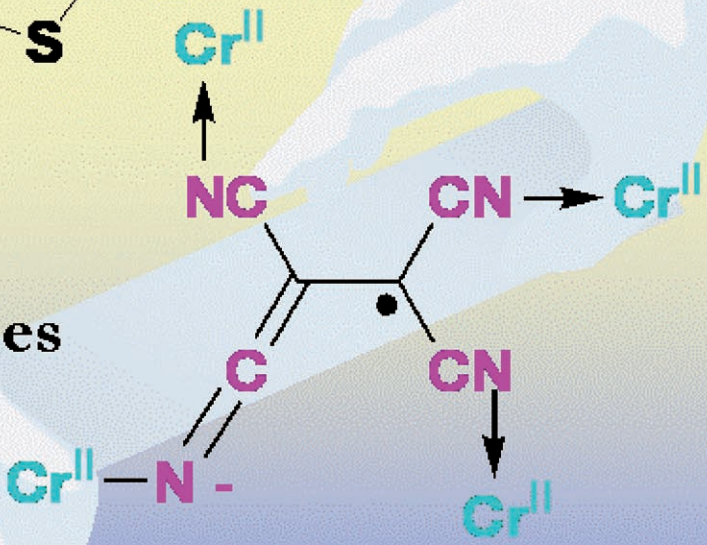

Solvated versus solvent-free phases

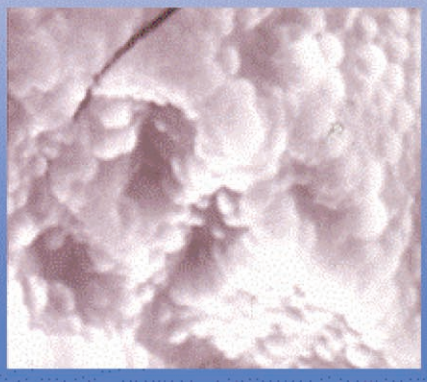

CVD films

Ligand Influence on Connectivity and Processing: Magnetic Crystals Based on Metalloceniums and Films of TCNE-Based Magnets (TCNE = Tetracyanoethylene)

Dominique de Caro, Christophe Faulmann, and Lydie Valade*[a]

Abstract: Molecular materials built from coordination complexes exhibit properties that can be explained through intermolecular electronic interactions driven by the ligand moieties. The nature of the ligand in the precursor molecules governs the connectivity of the magnetic phases and the possibility of producing them by using a gas-phase process. Metallocenium, metal bisdithiolate materials, and solvated and solvent-free [M(tcne)$_2$] (tcne = tetracyanoethylene) magnets illustrate such features.

Keywords: chemical vapor deposition · coordination modes · magnetic properties · molecular materials · thin films

Introduction

Molecular materials properties result from supramolecular features for which intermolecular interactions play a key role. When coordination complexes are used as building blocks, these interactions are driven by the ligands through electronic delocalization by using π–π interactions within stacks of molecules or atom-to-atom short contacts between stacks. This is a classical feature of molecular conductors and superconductors containing coordination complexes. Therefore, the ligand design should not only consider the coordinating atoms, but also the peripheral ones and their overall structural organization. Although magnetic properties of coordination complexes mainly arise from the nature of the metal, long-range phenomena, as present in molecular magnets, are stabilized if cooperativity appears within the material through the build up of spin networks. Therefore, in order to reach an efficient connectivity, the ligands for coordination complex building blocks should be adequately chosen to favour ferromagnetic interactions.[1,2]

In this paper, we illustrate the above features by describing two families of coordination complexes: 1) crystalline adducts containing metalloceniums and metal–dithiolate building blocks, and 2) polymeric [M(tcne)$_2$] phases.

The first section of the paper is dedicated to the first family, in which both the metallocenium and the metal–dithiolate complex can act as spin carriers. Let us note that, in addition to magnetic properties, the metal–dithiolate complexes can lead to conductive species upon partial oxidation. The discussion focuses on the variation of the magnetic properties of [MCp*$_2$][Ni(dithiolate)$_2$] upon changing the metallocenium nature (MCp*$_2$ with M = Co, Fe, Mn), and describe the consequences of the ligand nature on the structural and magnetic properties of the [MnCp*$_2$][Ni(dithiolate)$_2$] system when the dithiolate is either dmit ($C_3S_5^{2-}$: 1,3-dithiol-2-thione-4,5-dithiolate) or dmid ($C_3OS_4^{2-}$: 1,3-dithiol-2-one-4,5-dithiolato).

The second section of the paper concerns the [M(tcne)$_2$]·solvent family of magnets. In this section we discuss the ligand exchange mechanism involved in the formation of these solvated phases and the ligand–solvent competition at the vicinity of the metal centre, which, by reducing the spin-network dimensionality, induces a significant variation of the ordering temperatures (T_c) of the isolated phases.

Solving the problem of ligand–solvent competition is at the heart of the use of the solvent-free preparation technique described in the third part of the paper. Ligand-exchange-based reactions are classically applied for building new complexes. A more confidential application for coordination chemists is the use of such reactions for film processing through gas-phase transport by chemical vapour deposition (CVD), and in particular by the so-called OMCVD which uses organometallic (OM) precursors.[3] Moreover, these gas-phase conditions offer the advantage of perform-

[a] Dr. D. de Caro, Dr. C. Faulmann, Dr. L. Valade
Laboratoire de Chimie de Coordination
CNRS–UPR 8241, 205 route de Narbonne
31077 Toulouse Cedex 4 (France)
Fax: (+33) 561-553-003
E-mail: valade@lcc-toulouse.fr

ing chemical reactions in the absence of solvent, an important feature for $[M(tcne)_2]$ magnets, in which solvent molecules have the deleterious effect on T_c mentioned above. The precursor ligand role in OMCVD is described and its influence on the nature and properties of the grown phases is developed in the $[M(tcne)_2]$ case. Solvent free $[M(tcne)_2]$ (M = V, Cr, Mo, Nb) phases are described; they exhibit enhanced connectivity with respect to materials obtained from solution methods.

Metal–Dithiolate Complexes and Metalloceniums

Dithiolate ligands have been largely used as building bricks for preparing molecular materials exhibiting conductive, magnetic or optical properties.[4,5] In addition to potential magnetic properties, they are expected to form conductive networks in which electronic paths arise along molecular stacks. When associated with other magnetic species, they may create communication pathways between spin carriers. Following the pioneering study by Broderick et al.,[6] who investigated the $[FeCp^*_2][Ni(dmit)_2]$ compound, which exhibits ferromagnetic interactions down to 2.1 K, we have focused on the study of $[MCp^*_2][M'(dmit)_2]$ and $[MCp^*_2][M'(dmid)_2]$ ($dmit^{2-}$ = 1,3-dithiol-2-thione-4,5-dithiolate; $dmid^{2-}$ = 1,3-dithiol-2-one-4,5-dithiolato) adducts, in which both the metallocenium unit and the dithiolate ligand were varied.

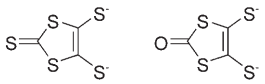

The magnetic properties of the $[MCp^*_2][Ni(dmit)_2]$ and $[MCp^*_2][Ni(dmid)_2]$ complexes studied are gathered in Table 1.

Upon partial oxidation of the metal–dithiolate unit of the 1:1 adduct, these materials may exhibit coupled conductive/magnetic properties. Before envisioning coupling of properties, the study of the 1:1 adduct was undertaken to better understand the nature of the interactions (ferro- or antiferromagnetic) between the building units in these complexes. It should be noted that $dmit^{2-}$ is not the sole ligand to enable ferromagnetic properties, since, among others, mnt^{2-} (maleonitriledithiolate), tfd^{2-} (bis(trifluoromethyl)ethylene dithiolate, also abbreviated as tdt^{2-}), and tds^{2-} (bis(trifluoromethyl)ethylene diselenolate) ligands also appear in several compounds exhibiting such properties.[10–16]

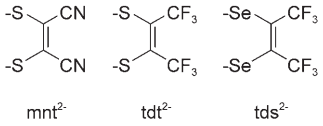

Metallocenium change: Following the idea proposed by Broderick et al. (use of a high-spin cation)[17] to enhance the magnetic properties of $[MCp^*_2][Ni(dithiolate)_2]$, we have substituted $[FeCp^*_2]^+$ for $[MnCp^*_2]^+$, and synthesized the $[MnCp^*_2][Ni(dmit)_2]$ adduct.[8,18] This compound exhibits almost exactly the same cell parameters and the same structural arrangement as the $[FeCp^*_2]$-derived complex. The overall structural arrangement consists of $\cdots D^+D^+A^-A^-D^+D^+A^-A^-\cdots$ stacks composed of side-by-side $[MnCp^*_2]^+$ ions alternating with face-to-face $[M(dmit)_2]^-$ ions, the latter forming slipped diads (Figure 1).

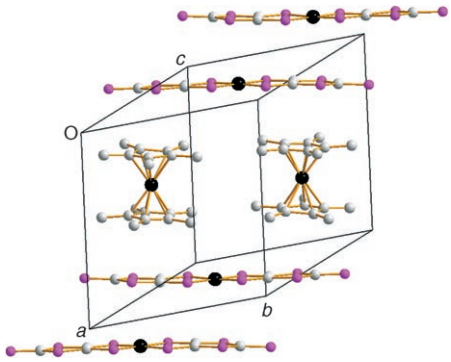

Figure 1. Structure of $[MnCp^*_2][Ni(dmit)_2]$ showing the $\cdots A^-A^-D^+D^+A^-A^-\cdots$ motif.

Table 1. Magnetic properties of $[MCp^*_2][Ni(dmit)_2]$ and $[MCp^*_2][Ni(dmid)_2]$ adducts.

	Magnetic properties[a]	θ/T_c [K]	Ref.	CCDC no.[b]
$[CoCp^*_2][Ni(dmit)_2]$	FM interactions	0.5	[7]	
$[FeCp^*_2][Ni(dmit)_2]$	FM interactions	2.1	[6]	
$[MnCp^*_2][Ni(dmit)_2]$	ferrimagnet	2.5	[8]	203647
$[FeCp^*_2][Ni(dmid)_2]\cdot THF$	FM interactions	10.5	[8]	
$[FeCp^*_2][Ni(dmid)_2]\cdot MeCN$	FM interactions	1.97	[9]	
$[MnCp^*_2][Ni(dmid)_2]\cdot MeCN$	FM interactions	2.8	[8]	203645
$[MnCp^*_2][Ni(dmid)_2]\cdot Me_2CO$	FM interactions	8.58	[7]	291582
$[MnCp^*_2]_2[Ni(dmid)_2]_2\cdot PhCN$	AFM interactions	−3.62	[7]	291583

[a] FM = ferromagnetic, AFM = antiferromagnetic. [b] CCDC numbers contain the supplementary crystallographic data (excluding structure factors) for these compounds. These data can be obtained free of charge from the Cambridge Crystallographic Data Centre via www.ccdc.cam.ac.uk/data_request/cif.

The magnetic properties of $[FeCp^*_2][Ni(dmit)_2]$ and $[MnCp^*_2][Ni(dmit)_2]$ are also similar, since both exhibit ferromagnetic interactions at low temperatures.[6,8] Nevertheless, the Mn compound exhibits a long-range magnetic order below 2.5 K,[8] which is not observed in the Fe-derived compound.[6] $[MnCp^*_2][Ni(dmit)_2]$ behaves like a ferrimagnet.

The change from Fe to Mn in the $[MCp^*_2]^+$ counterion has resulted in an improvement of the magnetic properties. Although the structures have been solved at different temperatures (RT for the Fe complex and 160 K for the Mn complex), data reported in Table 2 show that substitution of

Table 2. Selected shortest intermolecular distances [Å] within $[MCp^*_2][Ni(dmit)_2]$.

	$[MnCp^*_2][Ni(dmit)_2]$	$[FeCp^*_2][Ni(dmit)_2]$	difference
M–M	8.411(8)	8.412	0.001
Ni–Ni	5.574(8)	5.563	0.011
M–Ni	6.591(7), 7.330(8)	6.557, 7.299	0.034, 0.031

Fe for Mn in $[MCp^*_2]^+$ does not induce important changes in the intermolecular distances within these compounds.

Moreover, even if more short contacts are observed in the Mn compound than in the Fe one (29 versus 18, Figure 2),

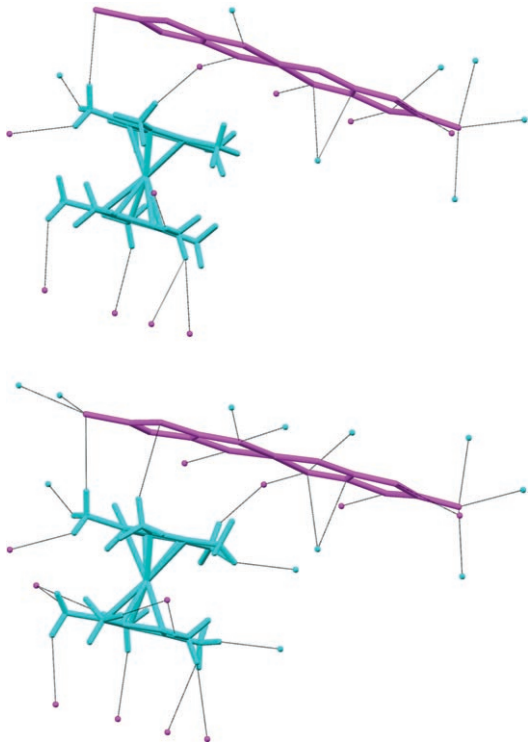

Figure 2. Short contacts (< sum of the van der Waals radii) in $[FeCp^*_2][Ni(dmit)_2]$ (top) and $[MnCp^*_2][Ni(dmit)_2]$ (bottom).

this should be related to the low-temperature structure determination of the Mn compound with respect to the RT structure determination of the Fe one. Therefore, since no significant structural change is observed between $[FeCp^*_2][Ni(dmit)_2]$ and $[MnCp^*_2][Ni(dmit)_2]$, the difference in the physical properties of these compounds arises only from the difference in the spin number of the metallocenium involved as counterion. However, it can be pointed out that the $[M(dmit)_2]$ complex fully plays its role of magnetic information exchanger between sites.

Dithiolate change: Another way to change the physical properties of $[MCp^*_2][M'(ligand)_2]$ compounds is to change the nature of the ligand. A "slight" modification of the $dmit^{2-}$ ligand can be made by changing the terminal S atom for an O atom. Substitution of the terminal C=S group for a C=O group in the $dmit^{2-}$ ligand affords the $dmid^{2-}$ ligand. It has already been shown that such a change in the ligand leads to complexes with different electrical properties.[4] This was partly explained by the electrochemical properties of the $[M(dmid)_2]$ complexes, which are different from those of the $[M(dmit)_2]$ complexes, and also by numerous differences in their structural arrangement.

By using $(n\text{-}Bu_4N)[Ni(dmid)_2]$ instead of $(n\text{-}Bu_4N)[Ni(dmit)_2]$ during the metathesis reaction with $[MnCp^*_2][PF_6]$ in acetonitrile or acetone affords isostructural compounds of general formula $[MnCp^*_2][Ni(dmid)_2]\cdot$solvent. The magnetic behaviour of $[MnCp^*_2][Ni(dmid)_2]\cdot CH_3CN$ is dominated by ferromagnetic interactions.[8] The structural arrangement of $[MnCp^*_2][Ni(dmid)_2]\cdot CH_3CN$ and $[MnCp^*_2][Ni(dmid)_2]\cdot (CH_3)_2CO$,[7] (Figure 3) is similar to that of $[FeCp^*_2][Ni(dmid)_2]\cdot CH_3CN$,[9] but different from that of $[MCp^*_2][Ni(dmit)_2]$ (M = Fe, Mn) (Figure 1). It is worth noting that, as for $[MCp^*_2][Ni(dmit)_2]$, the metallocenium change in $[MCp^*_2][Ni(dmid)_2]\cdot$solvent does not induce any change in the structural properties of the complexes. The overall structural arrangement consists of $\cdots D^+D^+A^-D^+D^+A^-\cdots$ mixed layers parallel to the *ab* plane and separated in the *c* direction by anionic sheets of $[Ni(dmid)_2]^-$ units, which are almost perpendicular to the mixed layers (Figure 3). The

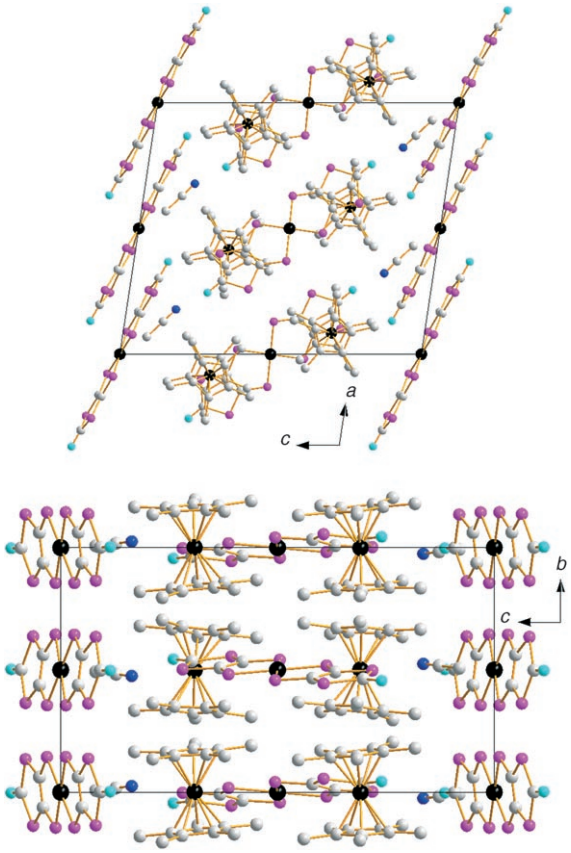

Figure 3. Structural arrangement of $[MnCp^*_2][Ni(dmid)_2]$. CHCN in the *ac* plane (top) and in the *bc* plane (bottom).

planes of the Cp* cycles are almost parallel to the planes of the $[Ni(dmid)_2]$ units in the mixed layers.

On the other hand, substitution of the terminal C=S group for the C=O group leads to complexes with different structural arrangements (Figure 3 versus Figure 1). As the structures are different, in order to relate physical properties to structural features it is only possible to compare the nature of atoms involved in intermolecular interactions and the number of such so-called contacts. Figure 4 shows the contacts between the various units in $[MnCp^*_2][Ni(dmit)_2]$ and in $[MnCp^*_2][Ni(dmid)_2]\cdot CH_3CN$.

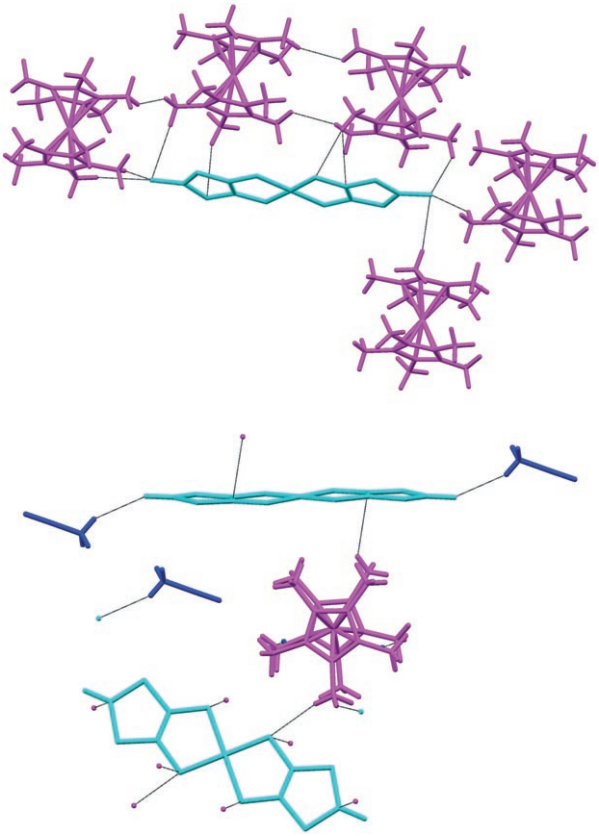

Figure 4. View of the short contacts within $[MnCp^*_2][Ni(dmit)_2]$ (top) and $[MnCp^*_2][Ni(dmid)_2]\cdot CH_3CN$ (bottom).

There are 29 short contacts in $[MnCp^*_2][Ni(dmit)_2]$; 16 are from the $[Ni(dmit)_2]^-$ units, among which six involve the terminal S atoms (Table 3). The latter are only directed towards H atoms of $[MnCp^*_2]^+$ (five units, Figure 4 top), and not towards other $[Ni(dmit)_2]^-$ units.

There are 16 short contacts in $[MnCp^*_2][Ni(dmid)_2]\cdot CH_3CN$. One $[Ni(dmid)_2]^-$ unit is connected to six $[MnCp^*_2]^+$ ions through eight contacts; the other $[Ni(dmid)_2]^-$ unit is connected (four contacts) to two solvent molecules through two contacts with the terminal C=O groups (Table 3), and to two $[MnCp^*_2]^+$ ions (two contacts).

The change from C=S to C=O results in the disappearance of 13 contacts between $[MnCp^*_2]^+$ and $[Ni(dmit)_2]^-$, in favour of interactions with the solvent (see next section).

Table 3. Contacts from the terminal X atom of the $[Ni(S_2C_2CX)_2]$ units in $[MnCp^*_2][Ni(dmit)_2]$ and $[MnCp^*_2][Ni(dmid)_2]\cdot$solvent.[a]

$[MnCp^*_2][Ni(dmit)_2]$			$[MnCp^*_2][Ni(dmid)_2]\cdot CH_3CN$		
Atom 1	Atom 2	Distance [Å]	Atom 1	Atom 2	Distance [Å]
S5	$H23B^1$	2.842	O1	$H30C^5$	2.481
S5	$H16A^2$	2.942	$O1^6$	$H30C^7$	2.481
S5	$H12C^3$	2.883			
S10	$H16C^4$	2.927			
S10	H23A	2.925			
S10	$H12A^4$	2.982			

[a] Symmetry operation to be applied 1: $1+x, 1+y, 1+z$; 2: $1+x, 1+y, z$; 3: $1-x, 1-y, 1-z$; 4: $1-x, -y, -z$; 5: $-1+x, y, z$; 6: $1-x, 1-y, -z$; 7: $2-x, 1-y, -z$.

The low polarity of the C=S group might explain its inclination to interact easily with slightly positively charged atoms (such as H of Cp* groups) rather than with H atoms of acetonitrile (which are much more positively charged due to the large dipolar moment of the cyano group).

Nevertheless, this loss of contacts does not forbid ferrimagnetic interactions within $[MnCp^*_2][Ni(dmid)_2]\cdot CH_3CN$.[7] However, long-range features are not observed, as this phase is not a ferrimagnet, unlike $[MnCp^*_2][Ni(dmit)_2]$.[8]

Influence of the solvent: The number of contacts is not the only key point for this kind of compound to behave like a ferrimagnet. Indeed, the $[MnCp^*_2][Ni(dmid)_2]\cdot$acetone,[7] synthesized by performing the metathesis reaction between $(n\text{-}Bu_4N)[Ni(dmid)_2]$ and $[MnCp^*_2][PF_6]$ in acetone instead of acetonitrile, exhibits 54 short contacts between its units (Figure 5, top), which is much more than the 29 observed in the $[MnCp^*_2][Ni(dmit)_2]$ ferrimagnet.[8]

In $[MnCp^*_2][Ni(dmid)_2]\cdot$acetone, the terminal O atoms of the $dmid^{2-}$ ligand are involved in 14 short contacts (Table 4). One $[Ni(dmid)_2]^-$ unit is connected to four $[MnCp^*_2]^+$ ions (2×3 contacts from its terminal O atoms) and the other $[Ni(dmid)_2]^-$ unit is connected to two solvent molecules, to two $[MnCp^*_2]^+$ ions and to two $[Ni(dmid)_2]^-$ ions (Figure 5, bottom). Despite of these numerous interactions, $[MnCp^*_2][Ni(dmid)_2]\cdot$acetone is not a ferrimagnet and only exhibits ferromagnetic interactions.

Actually, changing the terminal C=S group for a C=O group, that is going from the $dmit^{2-}$ ligand to the $dmid^{2-}$ ligand, in the metallocenium-containing compounds induces the inclusion of solvent molecules in the crystal structure. Indeed, most of $[M(dmid)_2]$ complexes associated with metalloceniums are solvated. This is also observed in $[FeCp^*_2][Ni(dmid)_2]\cdot$THF.[19] For only one series of compounds, that is, $[FeCp^*_2][M(dmid)_2]$, (M=Ni, Pd, Pt), once briefly reported,[20] is there no solvent molecule incorporated into the solid-state structure. However, to our knowledge, no data for these complexes are available in the Cambridge Structural Data Centre and they have never been fully reported in related papers. As stated above, this tendency to include solvent within the structure might be due to the larger polarity of the terminal C=O bond compared to that of the C=S bond: this larger polarity will favour interactions with the low electron density of polar solvents, such as acetonitrile,

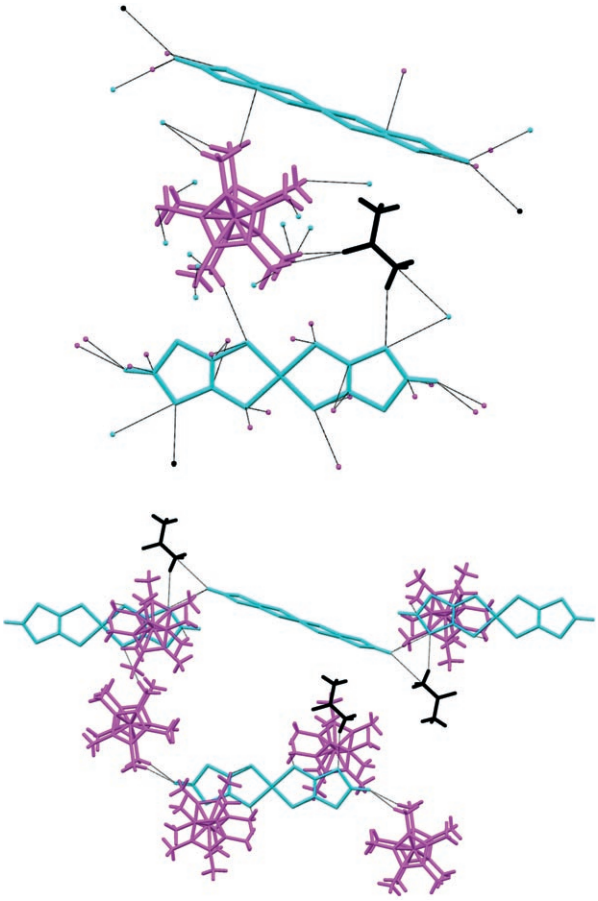

Figure 5. Contacts between units in $[MnCp^*_2][Ni(dmid)_2]\cdot(CH_3)_2CO$ (top) and from the O atoms of the $Ni(dmid)_2$ units (bottom).

Table 4. Contacts from the terminal O atom of the $[Ni(dmid)_2]$ units in $[MnCp^*_2][Ni(dmid)_2]$·acetone.

		Symmetry operation		Distance [Å]
Atom 1	Atom 2	on atom 1	on atom 2	
O1	S8	x, y, z	$1-x, 1-y, 1-z$	3.174
O1	S8	$1-x, 1-y, -z$	$x, y, -1+z$	3.174
O2	H23B	$2-x, 1-y, 1-z$	$1+x, y, z$	2.634
O2	H23B	x, y, z	$1-x, 1-y, 1-z$	2.634
O2	H12B	$2-x, 1-y, 1-z$	$1+x, y, z$	2.624
O2	H12B	x, y, z	$1-x, 1-y, 1-z$	2.624
O2	H26C	$2-x, 1-y, 1-z$	$1/2+x, 1/2-y, z$	2.699
O2	H26C	x, y, z	$1.5-x, 1/2+y, 1-z$	2.699
O1	C32	x, y, z	$-1+x, y, z$	3.186
O1	C32	$1-x, 1-y, -z$	$2-x, 1-y, -z$	3.186
O1	H13A	x, y, z	$-1/2+x, 1.5-y, z$	2.693
O1	H13A	$1-x, 1-y, -z$	$1.5-x, -1/2+y, -z$	2.693
H13A	O1	x, y, z	$1/2+x, 1.5-y, z$	2.693
C32	O1	x, y, z	$1+x, y, z$	3.186

by disadvantaging interactions with methyl groups of the Cp* units. In a similar vein, since acetone is less polar than acetonitrile, the six H atoms are slightly less "positive" than the three H atoms of acetonitrile. Therefore the C=O groups of the ligands can interact either with the H atoms of acetone, or with those of the Cp* units. From these observations, one might expect that ligands containing electronegative atoms at their periphery should afford compounds that include solvent molecules when combined with metallocenium. This is supported by other examples, such as compounds including complexes of the mnt^{2-} ligand (mnt^{2-} = maleonitriledithiolate), in which the terminal C=N groups have a polarity in between those of C=O and C=S groups. Indeed, some mnt^{2-} complexes with metallocenium are solvated (α-$[FeCp^*_2]_2[M(mnt)_2]_2\cdot 2CH_3CN$, M = Co, Fe),[21] whereas others are not ($[FeCp^*_2][M(mnt)_2]$, M = Ni, Pt, Co).[10,21] Numerous structures and magnetic behaviours are found for these compounds, indicating that the outer atoms of the ligand have no preference to interact either with the solvent or with the cations.

It should be pointed out that none of the complexes derived from the tdt^{2-} or the tds^{2-} ligands are solvated: $[FeCp^*_2][M(tdt)_2]$ (M = Ni, Pt),[10] $[MnCp^*_2][M(tds)_2]$ (M = Ni, Pd, Pt)[14] and $[FeCp^*_2][M(tds)_2]$ (M = Ni, Pt)[16] exhibit a "cation–anion–cation–anion" motif in their structural arrangement. Their magnetic properties are dominated by ferromagnetic interactions. The tdt^{2-} and tds^{2-} ligands contain terminal CF_3 groups, the polarity of which is very large, and one might expect solvent to interact with these groups. Actually, the analysis of their crystal structure shows that they strongly interact with the methyl groups of Cp*, creating a quite compact structure. Steric considerations might hinder the CF_3 groups from interacting with the solvent.

At this point, one might expect that, whatever the solvent (acetone, acetonitrile or THF), all $[MCp^*_2][M'(dmid)_2]$·solvent complexes exhibit the structural arrangement shown in Figure 3, whereas all $[MCp^*_2][M'(dmit)_2]$ complexes show stacks containing a $\cdots A^-A^-D^+D^+A^-A^-\cdots$ motif (Figure 1). Recently, synthesis in benzonitrile afforded the$[MnCp^*_2]_2[Ni(dmid)_2]_2\cdot C_6H_5CN$ complex,[22] the structural arrangement of which has never been observed before (Figure 6).

The overall structural arrangement of this compound consists in stacks of $[Ni(dmid)_2]^-$ dimers (totally eclipsed) separated by pairs of $[MnCp^*_2]^+$ ions, forming a $\cdots D^+D^+A^-A^-D^+D^+A^-A^-\cdots$ chain (Figure 6). The solvent lies almost perpendicular to the $[Ni(dmid)_2]^-$ units. This kind of

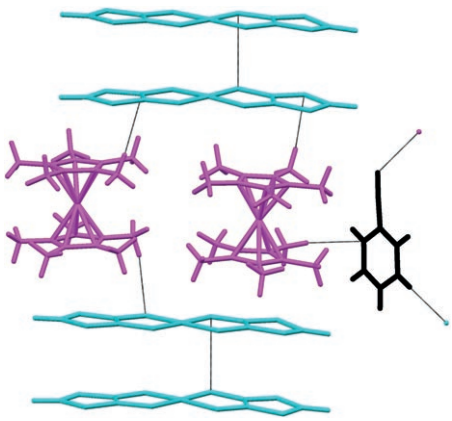

Figure 6. Structural arrangement in $[MnCp^*_2]_2[Ni(dmid)_2]_2\cdot C_6H_5CN$.

arrangement can be viewed as intermediate between that of $[MnCp^*_2][Ni(dmit)_2]$ (Figure 1) and that of $[MnCp^*_2][Ni(dmid)_2]\cdot CH_3CN$ (Figure 3). In this case, and opposite to the previous compounds with acetonitrile or acetone, the terminal C=O group of the $dmid^{2-}$ ligand does not interact with any other atoms. This compound exhibits antiferromagnetic interactions, due to strong antiferromagnetic coupling within the dimerized $[Ni(dmid)_2]$ units.

Concluding remarks on metal-dithiolate/metallocenium systems: The following conclusions can be drawn from the study of $[MCp^*_2][M'(dithiolate)_2]$ complexes.

- When a $[MnCp^*_2]^+$ ion ($S=1$) is substituted for a $[FeCp^*_2]^+$ ion ($S=^1/_2$), the change in metallocenium induces a spin density increase which, in turn, modifies the spin connectivity. $[MnCp^*_2][Ni(dmit)_2]$ is a ferrimagnet, while $[FeCp^*_2][Ni(dmit)_2]$ is not.
- The substitution of the terminal sulfur atom in $dmit^{2-}$ for an oxygen atom affords $dmid^{2-}$. This change modifies the structure of the compounds, but is not systematically accompanied with the reduction of the number of intermolecular interactions. The latter are related to the difference in polarity of the terminal C=O and C=S groups.
- Solvent molecules are part of the structure of $dmid^{2-}$ systems. They modify the structural arrangement and the spin network by preventing long-range interactions.

Solvated $[M(tcne)_2]$ Magnets

The first examples of such magnets were grown in solution, and solvent molecules always appear as part of their chemical structure.

Ligand exchange in the preparation of solvated $[M(tcne)_2]\cdot$solvent systems: Solvated $[M(tcne)_2]\cdot$solvent black magnetic phases have been extensively studied by J. S. Miller et al. (M: V, Mn, Fe, Co, Ni; tcne: tetracyanoethylene $(NC)_2C{=}C(CN)_2$).[23] They are prepared from the reaction of an organometallic precursor ($[V(C_6H_6)_2]$ or $[V(CO)_6]$) or MI_2 (M: Mn, Fe, Co, Ni) in the form of the CH_3CN solvate, and tcne. In the solid state $[Mn(tcne)_2]\cdot y\,CH_2Cl_2$ and $[Fe(tcne)_2]\cdot y\,CH_2Cl_2$ diffract and are isostructural, whereas $[Co(tcne)_2]\cdot y\,CH_2Cl_2$ and $[Ni(tcne)_2]\cdot y\,CH_2Cl_2$ poorly diffract and do not appear to be isomorphous to the manganese and iron analogues.[24] However, these patterns have yet to be indexed. The IR spectrum of the above $[M(tcne)_2]\cdot y\,CH_2Cl_2$ compounds exhibit two or three ν_{CN} absorptions, the width of which may depend on the precursor and experimental conditions. However, their positions (in the 2100–2240 cm^{-1} range) are consistent with those corresponding to a coordinated $[tcne]^{\bullet-}$ radical ion (Table 5). The synthesis of $[Cr(tcne)_x]\cdot y$solvent compounds was reported by using $[Cr(naphtalene)_2]$, $[Cr(NCCH_3)_4]^{2+}$ or $[Cr(NCCH_3)_6]^{2+}$ as starting complexes and tcne in either acetonitrile, dichloromethane, or toluene.[25] Whatever the starting complex, the Cr materials show strongly antiferromagnetic interactions between spin centres, but magnetic ordering was not observed. We have performed the preparation of the Nb/tcne derivative in toluene by using tcne and two different Nb starting complexes: $[Nb(i\mathrm{Pr}_2\text{-dad})_3]$ ($i\mathrm{Pr}_2$-dad: 1,4-diisopropyl-1,4-diazabuta-1,3-diene) and $[Nb(\eta^6\text{-mes})_2]$ (mes: mesitylene).[26] A low amount of black precipitate is obtained from $[Nb(i\mathrm{Pr}_2\text{-dad})_3]$ in refluxing toluene. Its IR spectrum evidences a strong band at 2199 cm^{-1} assigned to coordinated $[tcne]^{\bullet-}$ and the characteristic vibration modes of the diazabutadiene ligands, indicating an incomplete substitution of the $i\mathrm{Pr}_2$-dad ligand for tcne.

Table 5. Spectroscopic and magnetic characteristics of transition-metal/tcne systems.

Compound	ν_{CN} [cm^{-1}]	T_c [K]	Ref.
$[V(tcne)_2]\cdot y\,CH_2Cl_2$[a]	2189(s), 2153(s)	≈400	[23]
$[V(tcne)_2]\cdot 0.5\,CH_2Cl_2$[b]	2188(s), 2099(s)	≈400	[23]
$[Cr(tcne)_x]\cdot y\,C_6H_5CH_3$	2213(m), 2110(s)	[c]	[25]
$[Mn(tcne)_2]\cdot y\,CH_2Cl_2$	2224(m), 2181(s), 2171(s)	107	[24]
$[Fe(tcne)_2]\cdot y\,CH_2Cl_2$	2221(m), 2177(s), 2174(s)	121	[24]
$[Co(tcne)_2]\cdot y\,CH_2Cl_2$	2230 (m), 2187(s), 2167(s)	44	[24]
$[Ni(tcne)_2]\cdot y\,CH_2Cl_2$	2237(m), 2194(s)	44	[24]
$[Nb(tcne)_{1.1}]\cdot 0.4\,C_6H_5CH_3$	2198(s), 2092(s)	[d]	[26]

[a] From $[V(CO)_6]$. [b] From $[V(C_6H_6)_2]$. [c] The phase is not magnetic. [d] $H_c=200$ Oe at 2 K; signal too weak at 5 K.

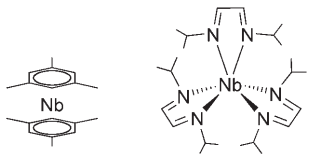

$[Nb(\eta^6\text{-mes})_2]$ $[Nb(i\mathrm{Pr}\text{-dad})_3]$

On the other hand, the reaction of $[Nb(\eta^6\text{-mes})_2]$ with tcne in toluene at room temperature leads instantaneously to a black precipitate, which was analyzed as $[Nb(tcne)_{1.1}]\,0.4\,C_7H_8$. Its IR spectrum in the ν_{CN} region exhibits two strong broad absorptions at 2198 and 2092 cm^{-1}, in agreement with coordinated $[tcne]^{\bullet-}$ species (Table 5). Moreover, preliminary magnetic measurements evidenced that this solvated compound exhibits a spontaneous magnetization at 2 K ($H_c=100$ Oe).

The reaction leading to $[M^{II}(tcne)_2]\cdot$solvent (M: Mn, Fe, Co, Ni) was conducted from solvated $M^{II}I_2$.[24] It can be postulated that the material results from the reduction of $tcne^0$ by I^- followed by complexation of M^{II} by $[tcne]^{\bullet-}$. The chelating effect of $[tcne]^{\bullet-}$ may explain the easy displacement of the monodentate I^- ligand and the stabilization of the $[M^{II}(tcne)_2]$ complex. In the case of the Fe derivative, the preparation of $[Fe^{II}(tcne)_2]\cdot CH_2Cl_2$ can be also performed by ligand exchange by reacting an Fe^{II} salt and a $[tcne]^{\bullet-}$ salt: $[Fe^{II}(NCMe)_4][B\{3,5\text{-}(CF_3)_2C_6H_3\}_4]_2$ and $(n\text{-}Bu_4N)$tcne in CH_2Cl_2.[24] However, reaction of $[V(C_6H_6)_2]$ or

$[V(CO)_6]$ with tcne did not proceed as expected. When reacting with tcne, $[V(C_6H_6)_2]$, which is isoelectronic with $[MnCp^*_2]$, was targeted to lead to $[V(C_6H_6)_2]^+[tcne]^{\bullet-}$ ($Mn^{II}Cp^*_2$ with tcne forms $[Mn^{III}Cp^*_2]^+[tcne]^{\bullet-}$). Also, the reaction of $[Cr(C_6H_6)_2]$ with tcne in solution affords the $[Cr(C_6H_6)_2]^+[tcne]^{\bullet-}$ phase.[27] We may postulate that the reactivity difference between $[V(C_6H_6)_2]$ and $[Cr(C_6H_6)_2]$ relies on the respective stability of the M^I intermediate species: the d^5 configuration of Cr^I corresponds to a half-filled shell giving a "special stability" to its complexes. The electrochemical properties of $[V(C_6H_6)_2]$ and $[Cr(C_6H_6)_2]$ have been reported in dimethoxyethane.[28] They show that $[Cr(C_6H_6)_2]$ is oxidized at a lower potential than $[V(C_6H_6)_2]$, $E_{1/2}(0/+) = -0.72$ and -0.35 V versus SCE, respectively. Moreover, irreversible second oxidation waves are found at $E_{pa} = +0.35$ and $+1.14$ V versus SCE for $[V(C_6H_6)_2]$ and $[Cr(C_6H_6)_2]$, respectively. These values indicate a larger stability domain for the $[Cr(C_6H_6)_2]^+$ monocationic species versus the $[V(C_6H_6)_2]^+$ ones. $[Cr(C_6H_6)_2]^+[tcne]^{\bullet-}$ is therefore stabilized with respect to $[V(C_6H_6)_2]^+[tcne]^{\bullet-}$. In the case of the niobium/tcne system, we have also mentioned above that $[tcne]^{\bullet-}$ displaces the η^6-mes ligand more easily than *i*Pr_2-dad. The respective bonding modes of the starting ligands may explain this result: Nb^0 is better stabilized by the bulky *i*Pr_2-dad ligand, which combines chelating, macrocyclic and π-delocalization effects, whereas only π-bonding effects are observed in the case of the η^6-mes ligand. Moreover, the Nb metal is more easily accessible for oxidation by tcne in the "sandwich" $[Nb(\eta^6\text{-mes})_2]$ complex than in $[Nb(i\text{Pr}_2\text{-dad})_3]$. Another example is given with the $[Mn(amtp)(CH_3CN)(tcne)_2]$ compound (amtp: tris(pyrazolylmethyl)-amine), in which the bulky amtp ligand is not de-coordinated when the $[Mn(amtp)(CH_3CN)][ClO_4]_2$ salt reacts with K[tcne].[29]

The formation of $[V(tcne)_2]\cdot$solvent from $[V(C_6H_6)_2]$ was more clearly understood through a mechanistic study that shows $[V(C_6H_6)_2]^{2+}$ species to be key intermediates in the process.[25] Considering the half-wave potentials of the $[tcne]^{\bullet-}/tcne^0$ and $[tcne]^{2-}/[tcne]^{\bullet-}$ systems ($+0.25$ and -0.79 V versus SCE, CH_2Cl_2),[30] oxidation of the $[V^0]$ species is anticipated to initially occur [Eq. (1)], and be followed by the disproportionation of the $[V^I]$ complex [Eq. (2)]. The formation of the $[V^{II}]$ complex may also result from a second oxidation step [Eq. (2′)] as the first reduction potential of tcne is very close to the irreversible oxidation of $[V^I]$ to $[V^{II}]$ (vide supra). The bis(benzene)vanadium(II) complex can then react with $[tcne]^{\bullet-}$ to form $[V(tcne)_2]$ according to Equation (3).

$$[V^0(C_6H_6)_2] + tcne^0 \rightarrow [V^I(C_6H_6)_2]^+ + [tcne]^{\cdot-} \quad (1)$$

$$2\,[V^I(C_6H_6)_2]^+ \rightarrow [V^0(C_6H_6)_2] + [V^{II}(C_6H_6)_2]^{2+} \quad (2)$$

$$[V^I(C_6H_6)_2]^+ + tcne^0 \rightarrow [V^{II}(C_6H_6)_2]^{2+} + [tcne]^{\cdot-} \quad (2')$$

$$[V^{II}(C_6H_6)_2]^{2+} + 2\,[tcne]^{\cdot-} \rightarrow [V^{II}(tcne^{\cdot-})_2] + 2\,C_6H_6 \quad (3)$$

Solvent effect on the properties of $M(tcne)_2$·solvent systems: Complex formation reactions are strongly solvent-dependent. The thermodynamic stability of a complex depends on the nature of the solvent, mainly because the solvation of all reactants in the system (both metal ions and ligands) competes with metal–ligand interactions. When $[V(tcne)_2]$ magnets are prepared in solution by using a coordinating solvent (e.g., CH_3CN, THF), $[V(C_6H_6)_2]^{2+}$ can also react with the solvent to form $[V(solvent)_6]^{2+}$ species [Eq. (4)]. This complex can lead more rapidly to $[V(tcne)_2]$ through the substitution of weakly coordinated solvent ligands for strong N-donor $[tcne]^{\bullet-}$ ligands [Eq. (5)].

$$[V^{II}(C_6H_6)_2]^{2+} + 6\,solvent \rightarrow [V^{II}(solvent)_6]^{2+} + 2\,C_6H_6 \quad (4)$$

$$[V^{II}(solvent)_6]^{2+} + 2\,[tcne]^{\cdot-} \rightarrow [V^{II}(tcne^{\cdot-})_2]\cdot solvent \quad (5)$$

However, depending on its coordinating ability, the solvent may either be innocent or remain in the final material by occupying metal coordination sites. The spin network is therefore modified and induces large changes in the T_c values. Table 6 gives the T_c values for $[V(tcne)_2]\cdot$solvent magnets when varying the solvent from a non-coordinating one, such as CH_2Cl_2, to a strongly coordinating one, such as CH_3CN.[31]

Table 6. Magnetic properties of $[V(tcne)_2]\cdot$solvent as a function of the solvent nature.

	T_c [K]	H_c [Oe]
$[V(tcne)_2]\cdot y\,CH_2Cl_2$	≈400	8 at 5 K; 60 at 300 K
$[V(tcne)_2]\cdot y$ THF	210	–
$[V(tcne)_2]\cdot y\,(CH_3CN/C_6H_6)$	140	–
$[V(tcne)_2]\cdot y\,CH_3CN$	100	0.15 at 50 K

In the presence of CH_2Cl_2, T_c is very high (≈400 K), whereas it decreases (210 K) when using THF, which can bind to V^{II} centres through its lone pair electrons located on the oxygen atom. In the presence of CH_3CN, the T_c value is significantly lowered (100 K), whereas this value is increased (140 K) when acetonitrile is diluted with a non-coordinating solvent (such as benzene). The authors postulate that:[31] "In $[V(tcne)_2]\cdot CH_2Cl_2$, dichloromethane is present as a spinless interstitial dopant. It will add disorder weakly to the exchange through superexchange and through van der Waals interactions with the unpaired spin orbitals. It will also perturb the anisotropy by changing the local symmetry. In $[V(tcne)_2]\cdot y\,CH_3CN$ and $[V(tcne)_2]\cdot y\,(CH_3CN/C_6H_6)$, acetonitrile acts as a spinless substitutional, as well as interstitial, dopant. Its effects on the exchange are through coordinating with the V^{II}, directly changing the occupancies of the unpaired spin orbitals. Replacement of a $[tcne]^{\bullet-}$ by an acetonitrile molecule breaks the local symmetry, inducing random anisotropy." Attempts to stabilize $[V(tcne)_2]\cdot$solvent by thermal treatment (to suppress the deleterious effect of solvent on T_c) led to a decrease in saturation magnetization values

and sometimes to the loss of long-range magnetic ordering.[23]

Concluding remarks on solvated [M(tcne)$_2$] magnets: We have seen that solvated [M(tcne)$_2$] magnets exhibit critical temperatures that depend on the metal and solvent nature. In the case of [V(tcne)$_2$]·0.5 CH_2Cl_2, as T_c exceeds room temperature, commercial applications can be envisioned, in magnetic shielding for instance. However, its very high sensitivity to air exposure constitutes an undeniable limitation to its use. Therefore, avoiding the use of solvent and obtaining stable [M(tcne)$_2$] materials in a practical usable form is of great interest. Preparation of solvent free phases can be performed by using chemical vapour deposition.

Solvent-Free [M(tcne)$_2$] Magnets

Generalities on chemical vapour deposition: Chemical vapour deposition (CVD) is typically applied for growing a solid material as a thin film on a substrate surface, by conducting a chemical reaction from gaseous starting compounds classically named as precursors.[3,32] CVD allows growing a large variety of materials such as metals, solid solutions, composite materials, and ceramic materials. OMCVD or MOCVD refer to the use of organometallic or metal–organic precursors, respectively. Organic CVD (OCVD) is also encountered in particular in the field of molecular materials studied as films for electronic or optical applications. Due to their lower thermal stability, organic, organometallic or metal–organic precursors allows conducting the CVD process at much lower temperatures than when inorganic precursors are used. As a consequence, polymer-like substrates may be treated, an important feature in plastic electronics. In the CVD process, precursors are vaporized and further transported towards the substrate surface by using a carrier gas. In the conventional thermally activated process, the substrate is heated at a temperature allowing the precursors to react and lead to the expected solid material. The material formation results from chemical reactions.

Ligand role in OMCVD: The chemical reaction arising on the substrate surface is most of the time a decomposition reaction followed by the nucleation and growth of the deposit. The formation of the deposit results from the succession of steps illustrated in Figure 7.

In order to induce surface growth, the substrate temperature is typically set higher than the gas-phase transport temperature. The quality and purity of the films rely on a careful choice of the precursor molecules. Typical precursor characteristics are gathered in Table 7.

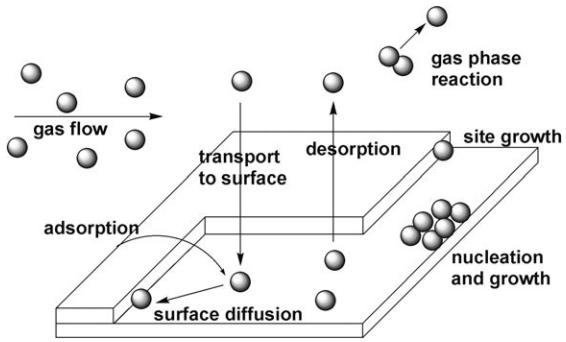

Figure 7. Succession of steps leading to film growth by chemical vapour deposition.[3]

When a coordination complex is used as a precursor, the ligand nature, lability and stability will fix the above characteristics. They will further govern the deposition conditions and, as a consequence, the nature and quality of the films. First, the volatility of the precursor depends on the degree of association of the molecules in the condensed state. Ionic complexes or molecules with ligands offering hydrogen-bonding possibilities generally exhibit low volatility. Secondly, the metal–ligand binding energy conditions the decomposition temperature. Electron-withdrawing groups are often added to lower the decomposition temperature. Ligands leading to volatile and thermally stable side-products avoid inclusion of impurities such as carbon, which is the most often encountered impurity. In some cases, the ligand may itself be source of one of the components of the desired material (e.g., for metal nitride or carbide formation). Illustrations of such features are numerous in the field of metal or ceramic deposits: the reader may consult the following references.[3,33–35]

CVD of molecular materials: Formation of molecular materials most often results from a reactive process corresponding to the association of building blocks within an adduct as, for example, in [TTF][TCNQ] (TTF = tetrathiafulvalene; TCNQ = tetracyano-*p*-quinodimethane) or [Fe(Cp*)$_2$][tcne] [Eqs. (6) and (7)].

$$TTF + TCNQ \rightarrow [TTF][TCNQ] \quad (6)$$

$$[Fe(Cp^*)_2] + tcne \rightarrow [Fe(Cp^*)_2][tcne] \quad (7)$$

Table 7. Precursors requirements for application in a CVD process.

Physicochemical properties	Thermal properties	Security and economical needs
good volatility high purity liquids preferred to solids (vaporization rate easier to stabilize, leads to constant growth rate and a better homogeneity of the deposit) good storage stability (low sensitivity to temperature, moisture or light)	good chemical stability at the vaporization temperature and during vapour transport low decomposition temperature clean reaction during film growth (side products should be volatile)	nontoxic precursors and side products non pyrophoric precursors and side products large availability at low cost (easy synthesis)

These materials have been grown by CVD following these reactions.[36,37] In such cases, and opposite to metal or ceramic deposition, decomposition of the precursors is not the basis of material formation, and should be avoided. Therefore, the substrate temperature is generally set lower than the vaporization temperature. This type of CVD reaction can be described as a reactive condensation. Sufficient energy has, however, to be transmitted 1) to the gas mixture in order to avoid condensation in the gas phase, and 2) to the substrate in order to initiate the reaction that would lead to the film growth on its surface.

CVD of films of $[M(tcne)_2]$ magnets can be considered as following a two-step mechanism combining a classical decomposition and a reactive condensation: 1) the decomposition of the metal precursor occurs with the loss of the ligand [Eq. (8)] and 2) a chemical reaction occurs between $tcne^0_{gas}$ and the M^0_{gas} leading to solid $[M^{II}(tcne)_2]$ [Eq. (9)]. Depending on the nature and number of the involved ligands, these two reactions may follow multi-step mechanisms.[3]

$$[M^0(L)_n]_{gas} \rightarrow M^0_{gas} + n\,L_{gas} \quad (8)$$

$$M^0_{gas} + 2\,tcne^0_{gas} \rightarrow [M^{II}(tcne^{\bullet -})_2]_{solid} \quad (9)$$

In addition to other criteria, in this case, the choice of the connecting ligand, as $[tcne]^{\bullet -}$, should take into account the properties expected in the new phase. Long-range magnetic properties will result from the ability of this ligand to favour spin interactions. The CVD technique has proved to be successful for preparing the new solvent-free $[M(tcne)_2]$ magnets gathered in Table 8.

Table 8. Properties of $[M(tcne)_2]$ phases prepared by CVD.

	ν_{CN} [cm^{-1}]	T_c [K]	H_c [Oe] (at T [K])
$[V(tcne)_2]$[a]	2214(m), 2191(m), 2158(s), 2124(sh), 2020(sh)	≈400	8.5 (5), 4 (300)
$[V(tcne)_2]$[b]	2192(m), 2105(s)	≈320	10 (5), 80 (300)
$[Cr(tcne)_2]$	2202(m), 2116(s)	–	100 (2.5), 80 (5), 70 (300)
$[Nb(tcne)_2]$	2200(s), 2180(sh), 2102(s)	–	200 (2)
$[Mo(tcne)_2]$	2212(s), 2113(m)	–	20 (2)

[a] From $[V(CO)_6]$. [b] From $[V(C_6H_6)_2]$.

Precursor influence in the CVD of the $[V(tcne)_2]$ room temperature magnet: $[V(tcne)_2]$ can be easily prepared at pressures around 200 Pa and relatively low deposition temperatures (≤75 °C) from gaseous tcne and $[V(C_6H_6)_2]$[37] or $[V(CO)_6]$[38] by using a conventional hot-wall CVD apparatus. Although very different V–C dissociation energies (4.26 eV for $[V(C_6H_6)_2]$ and 1.21 eV for $[V(CO)_6]$) in these two 17-electron organovanadium(0) complexes, electron transfer from the metal to tcne molecules and ligand exchange on the vanadium centre do occur. In both cases, saturation magnetization is in the 16–18 emu g^{-1} range at 5 K (consistent with antiferromagnetic coupling between $S=3/2$ V^{II} and two $S=1/2$ $[tcne]^{\bullet -}$ species) and follows a Bloch law with average exchange energies J/k_B in the 80–100 K range. However, room-temperature magnetic properties are significantly different. The room-temperature hysteresis loop of $[V(tcne)_2]$ prepared from $[V(C_6H_6)_2]$ shows a coercive field of $H_c=80$ Oe and a saturation magnetization of $M_s \approx 2.5$ emu g^{-1} (Figure 8). Values for $[V(tcne)_2]$ prepared from $[V(CO)_6]$ are $H_c=4$ Oe and $M_s \approx 0.6$ emu g^{-1}.

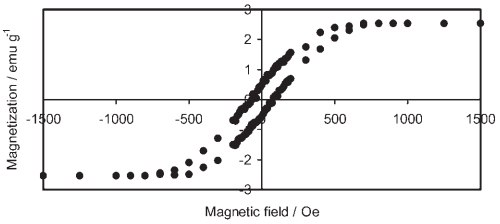

Figure 8. Hysteresis loop at 300 K for $[V(tcne)_2]$ deposit prepared from $V(C_6H_6)_2$.

To explain these differences, the coordination mode and the negative charge borne by tetracyanoethylene ligands have to be taken into account. The IR spectrum of $[V(tcne)_2]$ prepared from $[V(C_6H_6)_2]$ shows two ν_{CN} modes at 2192 (m) and 2105 cm^{-1} (s), in excellent agreement with monoreduced tcne moieties (i.e., $[tcne]^{\bullet -}$) bound to four vanadium atoms by means of σ–N bonds.[23] On the other hand, the IR spectrum of $[V(tcne)_2]$ prepared from $[V(CO)_6]$ exhibits, in the same region, five features at 2214 (m), 2191 (m), 2158 (s), 2124 (sh), and 2020 cm^{-1} (sh), indicating multiple coordination modes of $[tcne]^{\bullet -}$ and $[tcne]^{2-}$ species: $[tcne]^{\bullet -}$ as *trans*-μ-N, μ_n-$[tcne]^{\bullet -}$, μ_n-$[tcne]^{2-}$.[38,39] According to the ν_{CN} IR data, the authors postulate that the magnet is best formulated as $[V^{II}(tcne^{\bullet -})_x(tcne^{2-})_{1-x/2}]$ for $x<2$.[39] The presence of non magnetic $[tcne]^{2-}$ species in the composition of the phase is consistent with the lower value of the saturation magnetization. IR and room-temperature magnetic data for $[V^{II}(tcne^{\bullet -})_2]$ (obtained from $[V(C_6H_6)_2]$) are in excellent agreement with those for $[V(tcne)_2]\cdot 0.5\,CH_2Cl_2$ ($\nu_{CN}=2188$(m) and 2099 cm^{-1}(s); $H_c=60$ Oe and $M_s \approx 2.9$ emu g^{-1}) in which solvent molecules are non-coordinating.

This example perfectly illustrates the importance of the choice of the precursor molecules for performing CVD of $[M(tcne)_2]$ magnets. In the above mentioned case, the only difference is the nature of the ligand in the precursor: carbonyl or benzene. Following the proposed first step of material formation by CVD, that is the decomposition of the metal precursor [Eq. (6)], liberation of CO through the decomposition of $[V(CO)_6]$ affords a high reducing medium, while benzene issued from $[V(C_6H_6)_2]$ will be non-reactive. Therefore, from $[V(C_6H_6)_2]$, the electron transfer [Eq. (7)] only involves the metal and tcne, and leads to a material

combining M^{II} and $[tcne]^{\bullet-}$ entities. On the other hand, in the case of $[V(CO)_6]$, CO may participate in the electron transfer. The increased reducing ability of the gas-phase medium therefore explains the formation of the $[tcne]^{2-}$ entities evidenced by IR spectroscopy. A good choice of the precursor molecule, that is that of the ligand in the case of transition-metal complexes, may avoid the formation of undesired products or side-products. In the case of $[V(tcne)_2]$, we have seen that the magnetic performances of the phase at room temperature is much poorer when it contains tcne in two different oxidation states, than when only $[tcne]^{\bullet-}$ is present. A better control of the oxidation state of tcne was possible by using $[V(C_6H_6)_2]$.

Competing reactions—$[Cr(tcne)_2]$, an air-stable room-temperature magnet: The preparation of the chromium derivative by CVD was performed by using $[Cr(C_6H_6)_2]$ as the chromium source.[40] Although the Cr–C dissociation energy in the 18-electron complex (1.71 eV) is lower than that of V–C in $[V(C_6H_6)_2]$ (4.26 eV), loss of benzene rings is not observed at $T \leq 80\,^{\circ}C$. In the 40–80 °C temperature range, the reaction of gaseous $[Cr(C_6H_6)_2]$ and tcne leads to a purple deposit of $[Cr(C_6H_6)_2]^{+}[tcne]^{\bullet-}$ according to ν_{CN} bands (2191 (m), 2173 (s), and 2155 cm^{-1} (s)) which are identical to those of the solution-grown $[Cr(C_6H_6)_2]^{+}[tcne]^{\bullet-}$ compound. We have mentioned (vide supra) the larger stability towards oxidation in solution of the $[Cr(C_6H_6)_2]^{+}$ monocationic species relative to $[V(C_6H_6)_2]^{+}$. This feature implies that the solvated chromium phase is obtained at higher temperatures than the vanadium one. Similar feature occurs in the gas phase: complete loss of benzene rings can be achieved at 75 °C[37] from $[V(C_6H_6)_2]$, but only in the 80–100 °C temperature range from $[Cr(C_6H_6)_2]$.[40] Under the latter conditions, black thin films of $[Cr(tcne)_2]$ are obtained (Figure 9). The IR spectrum shows two broad ν_{CN} bands at

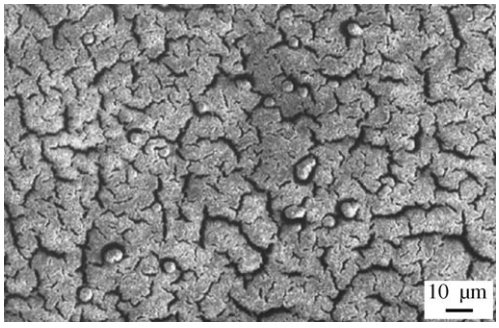

Figure 9. SEM image of a $[Cr(tcne)_2]$ deposit on silicon.

2116 (s) and 2202 cm^{-1} (m), consistent with $[tcne]^{\bullet-}$ ligands coordinated as μ_n-N–σ to the metal ($n = 2$–4). The X-ray photoelectron spectroscopy Cr $2p_{3/2}$ line has a binding energy at 576.3 eV, a typical value for Cr^{II} organometallic complexes, such as $[Cr(C_5H_5)_2]$. The films can be handled in air for ≈5 h. A longer exposure to air leads to free $tcne^0$ and chromium oxide formation.

Unlike solvated $[Cr(tcne)_x]\cdot y$ solvent complexes, which are not magnetically ordered above 2 K, as a thin film $[Cr(tcne)_2]$ behaves as a permanent magnet ($H_c = 100$ Oe at 2.5 K, 80 Oe at 5 K, 70 Oe at 300 K). The study of the chromium derivative clearly confirms again that, by both coordinating metal centres and creating structural disorder, solvent molecules prevent long-range magnetic ordering in $[M(tcne)_x]\cdot y$ solvent phases.

Stabilization of $[M(tcne)_2]$ magnets—structural studies: Unlike dichloromethane-prepared $[V(tcne)_2]\cdot 0.5\,CH_2Cl_2$, $[V(tcne)_2]$ films can be stabilized towards air exposure after annealing under a He atmosphere. Annealing is classically used either to increase the density and homogeneity of a material, or to induce solid-state chemical modifications that may afford specific bulk properties to the material.

We envisioned annealing $[V(tcne)_2]$ materials in order to increase the density the material. The initial deposit is made of small grains that coalesce upon heating. The coalescence process reduces the surface of material exposed to air and, as a consequence, its sensitivity towards oxygen. We observed that this thermal treatment reduces the saturation magnetization by a factor of about 40 ($M_s \approx 5.9 \times 10^{-2}$ emu g^{-1}). Upon air exposure, the annealed material still exhibits magnetic ordering at room temperature ($H_c =$ 50 Oe). However, reduction in the magnetization value by a factor of about five ($M_s \approx 1.2 \times 10^{-2}$ emu g^{-1}) is observed (with respect to the thermally treated sample kept under an argon atmosphere).

In the case of chromium, we have seen that two reactions are competing: oxidation versus decomposition of the metal precursor molecule. To orientate the reaction towards the $[Cr(tcne)_2]$ phase, a stronger thermal activation of the precursor is necessary with respect to that applied in the case of the vanadium derivative. On the other hand, this feature leads us to conclude that the chromium derivatives should exhibit better stability than the vanadium ones. Indeed, this phenomenon is observed: $[Cr(tcne)_2]$ is stable in air for about 5 h.

Most $[M(tcne)_2]$ magnets exhibit a polymer-like structure,[23] which cannot be determined by using classical X-ray diffraction techniques. The air stability of the chromium phase allowed us to perform the first structural study of a $[M(tcne)_2]$ magnet by using XANES and EXAFS techniques.[26] The principal characteristics of the chromium K-edge spectrum (XANES) show that the chromium atoms are located in an irregular octahedral environment. At the chromium K-edge, the Fourier transform of the EXAFS signal displays two peaks assigned to two shells around the chromium. They correspond to the nitrogen and carbon atoms of the tetracyanoethylene ligand. To extract information about the distances and the bond angles around the metallic atoms, we have modelled the EXAFS signal by using the FEFF7 code. The structural parameters that best fit with the experimental data are the following: six nitrogen neighbours around chromium, a mean Cr–N distance of 2.03 Å, a N–C distance of 1.30 Å and a ≈160 Cr-N-C angle.

It should be noted that the Cr–N distance in cyanato ($^-$N=C=O), thiocyanato ($^-$N=C=S) and alkylidineamido ($^-$N=CRR′) Cr^{III} complexes are in the 1.95–1.99 Å range.[41] In our case, a larger Cr–N distance suggests a lower oxidation state, that is, Cr^{II}, confirming X-ray photoelectron spectroscopy results.

More recently, complete XANES and EXAFS studies on $[V(tcne)_2]$ (prepared by gas-phase reaction of $[V(CO)_6]$ and tcne) have been reported.[42] As in the chromium case, two peaks are observed and assigned to dipole-forbidden 1s→3d transition (pre-edge) and to dipole-allowed 1s→4p transition. Interpretation of XANES data yields a valence state for V of 2.25 ± 0.25. A local slightly distorted octahedral environment is postulated. The V–N distance is 2.084 Å. This is 0.03 Å shorter than that reported for the model compound $[V(NCCH_3)_6]^{2+}$, indicating that $[V(tcne)_2]$ has more V–N back-bonding and has a stronger V–N bond than $[V(NCCH_3)_6]^{2+}$. The authors focus on the fact that the local environment is well defined with a distribution of V–N bond lengths comparable to that commonly found in ordered compounds. The small disorder in V–N distances (vibrational in origin) is a consequence of strong binding between V and tcne, with an effective local constant force of $k = 87\ N\,m^{-1}$. This strong bonding leads to strong nearest neighbour coupling, which for the extended structure of $[V(tcne)_2]$ with six N nearest neighbours results in magnetic ordering above room temperature.

Second-row transition metals—$Nb(tcne)_2$ and $Mo(tcne)_2$ low-temperature magnets: To our knowledge, we were the first to describe the syntheses of $[M(tcne)_x]\cdot y$ solvent and $[M(tcne)_2]$ systems with second-row transition metals. Following the results obtained in solution, the $[Nb(\eta^6\text{-mes})_2]$ complex seemed to be the precursor of choice for growing thin films of $[Nb(tcne)_2]$ by using the CVD technique. Although vaporization of the $[Nb(\eta^6\text{-mes})_2]$ precursor was efficient, no deposit was obtained, at least in the explored conditions. However, thin films of $[Nb(tcne)_2]$ could be obtained by using the $[Nb(i\text{Pr}_2\text{-dad})_3]$ precursor (deposition temperature: 80 °C; ≈1 μm polygonal grains).[43] The IR spectra of the films exhibit three ν_{CN} bands at 2200 (s), 2180 (sh) and 2102 cm^{-1} (s). These bands are in agreement with the presence of reduced tetracyanoethylene moieties bound to Nb. The N 1s X-ray photoelectron spectrum has two components at 398.1 and 399.9 eV assigned to nitrogen atoms in $[tcne]^{\bullet -}$ bound to Nb and to nitrogen atoms of free $tcne^0$, respectively. XPS analyses also evidence that the Nb $3d_{5/2}$ and Nb $3d_{3/2}$ lines are split into two components at 204.4, 206.3, 207.2, and 209.2 eV. The 204.4 and 207.2 eV peaks (60 %) are attributed to Nb^{II} by comparison with XPS data related to Nb^{2+} ions implanted into sapphire.[44] The other peaks (40 %) correspond to NbO_2, the presence of which is assigned to surface oxidation caused by handling the samples in the air before XPS measurements. After a bombardment of the films by Ar^+ ions for 15 min, which allows the removal of the surface oxide, the XPS spectrum then clearly shows two peaks (areas ratio: 1.50, as expected) corresponding to the $3d_{5/2}$ (204.6 eV) and $3d_{3/2}$ (207.4 eV) levels of Nb^{II}. Moreover, magnetic measurements evidence that the films exhibit a spontaneous magnetization at 2 K ($H_c = 200$ Oe).

Thin films of $[Mo(tcne)_2]$ were prepared through chemical vapour deposition from $Mo(C_6H_5CH_3)_2$ and tcne precursors.[45] It should be pointed out that the morphology of the films is temperature dependent, higher temperatures favouring the coalescence of small grains into large platelets: worm-like fibres are obtained at 80 °C, roughly spherical grains grow at 100 °C and large square-shaped plates form at 120 °C (Figure 10).

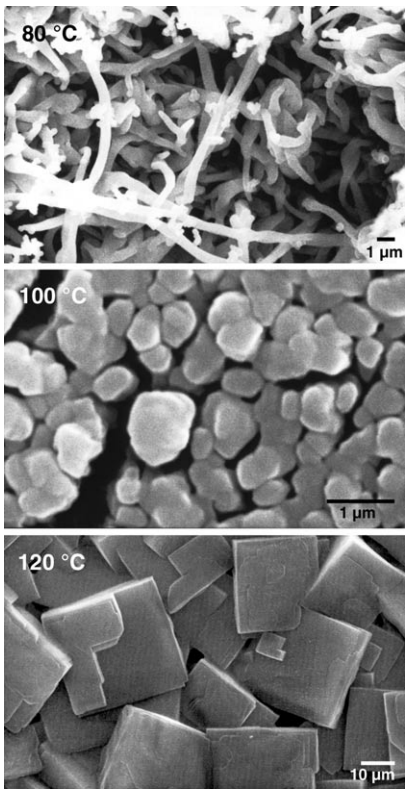

Figure 10. SEM images of $[Mo(tcne)_2]$ films deposited at 80 °C, 100 °C and 120 °C on silicon.

The XPS Mo $3d_{5/2}$ and Mo $3d_{3/2}$ lines are located at 228.7 and 231.8 eV, respectively (areas ratio: 1.33, in reasonable agreement with the theoretical value of 6:4). The Mo $3d_{5/2}$ has a binding energy very close to that for Mo^{II} complexes, such as $[Mo(C_5H_5)(CO)_3Cl]$ (228.7 eV) and $[Mo(C_5H_5)(CO)_3(SnMe_3)]$ (228.5 eV).[46] The N 1s signal (399.2 eV) has a binding energy consistent with the presence of $[tcne]^{\bullet -}$. This value is in good agreement with that obtained for $[Mn^{III}(tpp)][tcne]\cdot 2\,C_6H_5CH_3$ (tpp = *meso*-tetraphenylporphyrin), that is, 399.1 eV (*trans*-μ-$[tcne]^{\bullet -}$ moiety).[47] IR spectra show two ν_{CN} broad bands at 2212 (s) and 2113 cm^{-1} (m), close to those observed for $[Mn(C_5Me_5)(CO)_2][tcne]$ (2205 and 2125 cm^{-1}) in which tetracyanoethylene is *trans*-μ-N-bound to manganese(II). Moreover, no ν_{CH} bands (3070–2800 cm^{-1} region) corresponding

to the presence of toluene rings are observed. As in the niobium case, magnetic measurements evidence that the films exhibit a spontaneous magnetization at 2 K (H_c = 20 Oe). For temperatures higher than 2 K, magnetization values for both [Nb(tcne)$_2$] and [Mo(tcne)$_2$] were too low to be interpreted.

Both materials may contain remaining ligands issuing from an incomplete decomposition of their precursor. These remaining ligands have the same negative influence on magnetic properties as solvent molecules in [M(tcne)$_2$]·solvent phases: they prevent long-range magnetic ordering to occur at high temperatures.

Concluding remarks on the synthesis conditions versus magnetic properties of M/tcne systems: When a solvent-free technique such as CVD is applied to prepare [M(tcne)$_2$] magnets, the chance to reach systems exhibiting enhanced magnetic properties is greater than by applying solution based methods because:

- In CVD, under conditions for efficient decomposition of the metal precursor, tcne is easily reduced by M^0, and all coordination sites of the metal are available for the formed $[tcne]^{\bullet-}$ ligand to bind, while, in solution, M^{II}–$[tcne]^{\bullet-}$ interactions may compete with M^{II}–solvent interactions.
- As all coordination sites may be used, a three-dimensional network built on tcne connected by metal atom is favoured.
- The increased possibility of high-dimension networks explains that long-range magnetic interactions are encountered at higher temperatures in the solvent-free phases than in solvated ones.

In fact, solvent-free techniques allow the ligand that is chosen to play the role of a connector between spins, to "operate" in the best conditions. The better the network organization and regularity, the higher the magnetic performances.

Conclusion

Ligand nature has a tremendous effect on the build up of magnetic networks in molecular materials in the solid state. Ligands act as connectors between magnetic sites through π-delocalization effects and electronic interactions between peripheral atoms. Interligand interactions dictate the structural arrangement of the material. When preparations are conducted in solution, solvent molecules may either act as ligands or occupy interstitial sites. Both situations result in the break of the magnetic exchange. The solvent-free CVD method avoids this problem and affords possibility of isolating new phases.

Acknowledgements

The authors acknowledge J. Fraxedas for XPS data, F. Villain for EXAFS/XANES studies, M. Etienne for supplying Nb precursors, E. Rivière, A. Mari and J. F. Meunier for magnetic measurements, CNRS and Université Paul Sabatier for financial supports, and all the COST D14-3 community for fruitful exchange.

[1] C. J. Elsevier, J. Reedijk, P. H. Walton, M. D. Ward, *Dalton Trans.* **2003**, 1869–1880.
[2] M. Quesada, P. de Hoog, P. Gamez, O. Roubeau, G. Aromi, B. Donnadieu, C. Massera, M. Lutz, A. L. Spek, J. Reedijk, *Eur. J. Inorg. Chem.* **2006**, 1353–1361.
[3] F. Teyssandier, A. Dollet in *Non-equilibrium Processing of Materials, Vol. 10* (Ed.: C. Suryanarayana), Pergamon, Amsterdam, **1999**, pp. 257–285.
[4] C. Faulmann, P. Cassoux in *Dithiolene Chemistry. Synthesis, Properties, and Applications, Vol. 52* (Ed.: E. I. Stiefel), Wiley, Hoboken, New-Jersey, **2004**, pp. 399–489.
[5] N. Robertson, L. Cronin, *Coord. Chem. Rev.* **2002**, *227*, 93–127.
[6] W. E. Broderick, J. A. Thompson, M. R. Godfrey, M. Sabat, B. M. Hoffman, *J. Am. Chem. Soc.* **1989**, *111*, 7656–7657.
[7] C. Faulmann, S. Dorbes, E. Riviere, A. Andase, P. Cassoux, L. Valade, *Inorg. Chim. Acta* **2006**, *359*, 4317–4325.
[8] C. Faulmann, E. Rivière, S. Dorbes, F. Senocq, E. Coronado, P. Cassoux, *Eur. J. Inorg. Chem.* **2003**, 2880–2888.
[9] M. Fettouhi, L. Ouahab, E. Codjovi, O. Kahn, *Mol. Cryst. Liq. Cryst.* **1995**, *273*, 29–33.
[10] J. S. Miller, J. C. Calabrese, A. J. Epstein, *Inorg. Chem.* **1989**, *28*, 4230–4238.
[11] S. Zürcher, V. Gramlich, D. von Arx, A. Togni, *Inorg. Chem.* **1998**, *37*, 4015–4021.
[12] M. Yamashita, K. Ono, S. Tanaka, K. Imaeda, H. Inokuchi, *Adv. Mater.* **1994**, *6*, 295–298.
[13] W. B. Heuer, P. Mountford, M. L. H. Green, S. G. Bott, D. O'Hare, J. S. Miller, *Chem. Mater.* **1990**, *2*, 764–772.
[14] W. E. Broderick, J. A. Thompson, B. M. Hoffman, *Inorg. Chem.* **1991**, *30*, 2958–2960.
[15] X. M. Ren, S. Nishihara, T. Akutagawa, S. Noro, T. Nakamura, W. Fujita, K. Awaga, Z. P. Ni, J. L. Xie, Q. J. Meng, R. K. Kremer, *Dalton Trans.* **2006**, 1988–1994.
[16] S. Rabaca, R. Meira, L. C. J. Pereira, M. Teresa Duarte, J. J. Novoa, V. Gama, *Inorg. Chim. Acta* **2001**, *326*, 89–100.
[17] W. E. Broderick, J. A. Thompson, E. P. Day, B. M. Hoffman, **1990**, *249*, 401–403.
[18] C. Faulmann, A. E. Pullen, E. Rivière, Y. Journaux, L. Retailleau, P. Cassoux, *Synth. Met.* **1999**, *103*, 2296–2297.
[19] S. Rabaca, I. C. Santos, M. T. Duarte, V. Gama, *Synth. Met.* **2003**, *135–136*, 695–696.
[20] S. Rabaca, V. Gama, D. Belo, I. C. Santos, M. T. Duarte, *Synth. Met.* **1999**, *103*, 2302–2303.
[21] M. Fettouhi, L. Ouahab, M. Hagiwara, E. Codjovi, O. Kahn, H. Constant-Machado, F. Varret, *Inorg. Chem.* **1995**, *34*, 4152–4159.
[22] CCDC-291583 contains the supplementary crystallographic data for this paper. These data can be obtained free of charge from The Cambridge Crystallographic Data Centre via www.ccdc.cam.ac.uk/data_request/cif.
[23] J. S. Miller, A. J. Epstein, *Chem. Commun.* **1998**, 1319–1325.
[24] J. Zhang, J. Ensling, V. Ksenofontov, P. Gütlich, A. J. Epstein, J. S. Miller, *Angew. Chem.* **1998**, *110*, 676–679; *Angew. Chem. Int. Ed.* **1998**, *37*, 657–660.
[25] D. C. Gordon, L. Deakin, A. M. Arif, J. S. Miller, *J. Am. Chem. Soc.* **2000**, *122*, 290–299.
[26] D. de Caro, M. Basso-Bert, H. Casellas, M. Elgaddari, J.-P. Savy, J.-F. Lamère, A. Bachelier, C. Faulmann, I. Malfant, M. Etienne, L. Valade, *C. R. Chimie* **2005**, *8*, 1156–1173.
[27] J. S. Miller, D. M. O'Hare, A. Chakraborty, A. J. Epstein, *J. Am. Chem. Soc.* **1989**, *111*, 7853–7860.

[28] C. Elschenbroich, E. Bilger, B. Metz, *Organometallics* **1991**, *10*, 2823–2827.
[29] G. B. Wang, H. F. Zhu, J. A. Fan, C. Slebodnick, G. T. Yee, *Inorg. Chem.* **2006**, *45*, 1406–1408.
[30] S. Lo Shiavo, G. Bruno, P. Zanello, F. Laschi, P. Piraino, *Inorg. Chem.* **1997**, *36*, 1004–1012.
[31] B. G. Morin, C. Hahm, J. S. Miller, A. J. Epstein, *J. Appl. Phys.* **1994**, *75*, 5782–5784.
[32] "Organic Conductors, Superconductors and Magnets: From synthesis to Molecular Electronics": L. Valade, D. de Caro, I. Malfant, *NATO Sci. Ser. II* **2004**, *139*, 241–268.
[33] H. D. Kaesz, R. S. Williams, R. F. Hicks, J. I. Zink, Y.-J. Chen, H.-J. Müller, Z. Xue, D. Xu, D. K. Shuh, Y. Kwan Kim, *New J. Chem.* **1990**, *14*, 527–534.
[34] L. Brissonneau, C. Valhas, *Ann. Chim.* **2000**, *25*, 81–90.
[35] H. Choi, S. Park, T. H. Kim, *Chem. Mater.* **2003**, *15*, 3735–3738.
[36] D. de Caro, J. Sakah, M. Basso-Bert, C. Faulmann, J.-P. Legros, T. Ondarcuhu, C. Joachim, L. Aries, L. Valade, P. Cassoux, *C. R. Acad. Sci. Ser. II* **2000**, *3*, 675–680.
[37] D. de Caro, M. Basso-Bert, J. Sakah, H. Casellas, J.-P. Legros, L. Valade, P. Cassoux, *Chem. Mater.* **2000**, *12*, 587–589.
[38] K. I. Pokhodnia, A. J. Epstein, J. S. Miller, *Adv. Mater.* **2000**, *12*, 410–413.
[39] J. S. Miller, *Inorg. Chem.* **2000**, *39*, 4392–4408.
[40] H. Casellas, D. de Caro, L. Valade, P. Cassoux, *Chem. Vap. Deposition* **2002**, *8*, 145–147.
[41] A. G. Orpen, L. Brammer, F. H. Allen, O. Kennard, D. G. Watson, R. Taylor, *J. Chem. Soc. Dalton Trans.* **1989**, *12*, S1-S83.
[42] D. Haskel, Z. Islam, J. Lang, C. Kmety, G. Srajer, K. I. Pokhodnya, A. J. Epstein, J. S. Miller, *Phys. Rev. B* **2004**, *70*, 054422.
[43] E. Lamouroux, E. Alric, H. Casellas, L. Valade, D. de Caro, M. Etienne, D. Gatteschi, *Electrochem. Soc. Proc.* **2003**, *8*, 1040–1046.
[44] N. K. Huang, B. Tsuchiga, K. Neubeck, S. Yamamoto, K. Narumi, Y. Aoki, H. Abe, A. Miyashita, H. Ohno, H. Naramoto, *Nucl. Instrum. Methods Phys. Res. Sect. B* **1998**, *143*, 479.
[45] E. Lamouroux, D. de Caro, L. Valade, *Thin Solid Films* **2004**, *467*, 93–97.
[46] S. O. Grim, L. J. Matienzo, *Inorg. Chem.* **1975**, *14*, 1014–1018.
[47] K.-i. Sugiura, S. Mikami, K. Iwasaki, S. Hino, E. Asato, Y. Sakata, *J. Mater. Chem.* **2000**, *10*, 315–319.

Published online: January 22, 2007

